Situation Prediction And Reaction Control (SPARC)

(Patent Pending)

M. Ruf[*†] J. R. Ziehn[*‡§]

B. Rosenhahn[‡] J. Beyerer[*†] D. Willersinn[*] H. Gotzig[¶]

Abstract:

Approaches to automated driving typically hand over vehicle control to specialized modules for intersection handling, parking, obstacle avoidance etc., depending on the perceived traffic situation. This paper proposes a continuous-state alternative that allows to take all modeled goals and influences into account simultaneously, similarly to how a human driver would behave. A dynamic map of the environment is analyzed in real time for traffic rules and obstacles. The behavior of dynamic objects is predicted into the near future. This information is used to generate a 3D penalty map over space and time. An optimal trajectory is found based on these penalties as well as on penalties for internal control parameters. This holistic approach considers all relevant goals as well as the dynamic limits of the ego vehicle simultaneously when planning the trajectory, and requires no sharp state transitions during operation.

Keywords: Fully automated driving, prediction, situation analysis, trajectory planning

1 Overview

The concept presented here is based on [14] and is limited to the situation interpretation and maneuver planning / execution tasks of autonomous driving. It relies on processed sensor information: A dynamic map with objects detected around the ego vehicle, along with stochastic measures of uncertainty for all observations, is assumed to exist.

This paper introduces a two-step concept for autonomous driving, *situation prediction* and *reaction control*, short SPARC. Given the information in the dynamic map, the SPARC concept performs the following steps (cf. Fig. 1):

1. Use navigation instructions and static map to place the next waypoints for the ego vehicle (cf. Fig. 2(a, bottom)).

[*]Fraunhofer Institute of Optronics, System Technologies and Image Exploitation (IOSB), 76131 Karlsruhe, {miriam.ruf, jens.ziehn, dieter.willersinn, juergen.beyerer}@iosb.fraunhofer.de

[†]Vision and Fusion Laboratory (IES), Institute for Anthropomatics, Karlsruhe Institute of Technology (KIT), 76131 Karlsruhe, miriam.ruf@kit.edu

[‡]{rosenhahn, ziehn}@tnt.uni-hannover.de, Institut für Informationsverarbeitung (TNT), Leibniz Universität Hannover, 30167 Hanover

[§]Corresponding author

[¶]heinrich.gotzig@valeo.com, Valeo Schalter und Sensoren GmbH

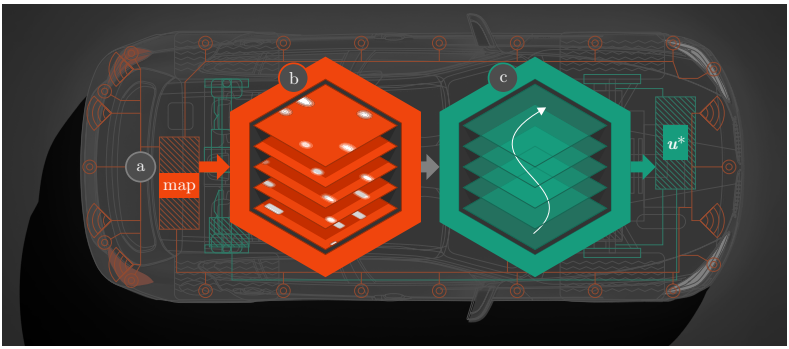

Figure 1: Outline of the proposed SPARC concept. The ego vehicle (a) sends a map of processed sensor information to the *situation prediction* block (b) that analyzes the scene and produces the holistic representation $\mathbf{H}$. The resulting *penalties* are passed to the *reaction control* block (c), which finds an optimal trajectory $\boldsymbol{\xi}^*$ and the corresponding control parameters $\boldsymbol{u}^*$. These are eventually fed back to the ego vehicle (a).

2. Derive information about static traffic rules (e.g. speed limits; not presented here) and assign *penalties* for their violation (cf. Fig. 2(a, top)).

3. Compute current (t_0) occupancy probabilities for spatial locations and assign penalties for their traversal (cf. Fig. 2(a, middle)).

4. Predict occupancies for $\{t_1, \ldots, t_{\max}\}$ and assign penalties (cf. Fig. 2(b)).

5. Find an optimal trajectory that approximately connects the waypoints based on the hard constraint of physical feasibility and the soft constraint of minimizing the sum of the following penalties (cf. Fig. 2(c)):

   - collisions (higher penalties: more severe collisions or more likely collisions)
   - traffic rule violations (higher penalties: more severe violations)
   - dynamics (higher penalties: uneconomic or uncomfortable driving)
   - deviations (higher penalties: wide offset from waypoints)

6. Estimate control commands until $t_{\max} \approx 5\,\text{sec}$, but recompute the trajectory much more frequently ($\approx 10\,\text{Hz}$) and only pass the very next set of control commands to the ego vehicle. Thus, the planning up to $t_{\max}$ is not intended to just bridge the gap between updates but to prevent decisions that will lead to ill states in the (relatively) far future. Furthermore, planning ahead can serve to bring the ego vehicle into a safe state upon total or partial sensor failure given the best last estimate.

The SPARC concept proposes a scalar or vector field over space and time, $\mathbf{H}(x, y, t)$, to store known and predicted information about the environment (the *holistic representation*,

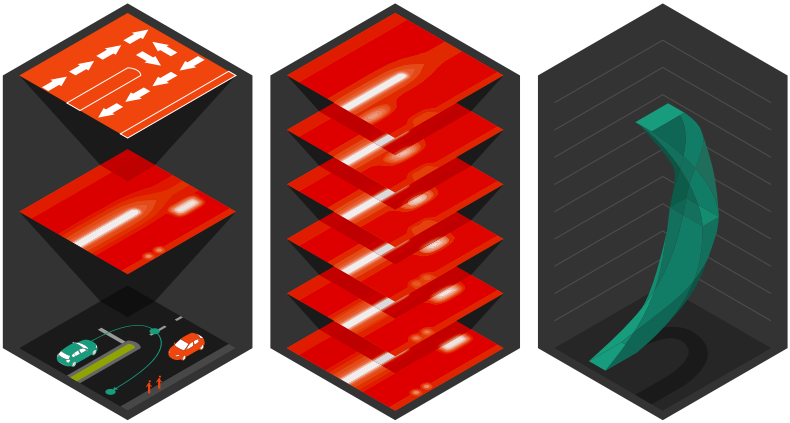

(a) (b) (c)

Figure 2: Elements of trajectory planning. (a) Bottom: Dynamic and static map of the scene, showing the ego vehicle (green) along with another car and two pedestrians (all red). The planned path $\boldsymbol{\xi}$ is indicated along with two waypoints. Middle: $\mathbf{H}$ at current collision risks, taking into account uncertainties in measurements. Top: $\mathbf{H}(x, y, t_{\text{now}})$ at traffic rules (admissible flow directions). (b) $\mathbf{H}(x, y, t_{\text{now}} \ldots t_{\text{max}})$ at prediction, showing the future development of the scene with growing uncertainties. (c) Planned trajectory $\boldsymbol{\xi}$ with ego vehicle footprint Φ wrapped around it to produce $\Phi \circ \boldsymbol{\xi}$. The penalties contained within the green volume determine the expected detriment of the passage.

cf. Fig. 2). Given a functional that evaluates the total penalty $\mathcal{P}[\,\boldsymbol{\xi}\,|\,\mathbf{H}\,]$ of a trajectory $\boldsymbol{\xi}$ given $\mathbf{H}$, the goal of finding the *optimal* trajectory $\boldsymbol{\xi}^*$ can be defined formally as

$$\boldsymbol{\xi}^* = \arg\min_{\boldsymbol{\xi}} \mathcal{P}[\,\boldsymbol{\xi}\,|\,\mathbf{H}\,] \tag{1}$$

Practically $\boldsymbol{\xi}^*$ has to be approximated using numerical techniques, and the computations of $\mathcal{P}$ in general and $\mathbf{H}$ in particular have to trade off between accuracy and computation time. Approaches to both based on the current progress of development are presented here.

2 State of the Art and Motivation

The most well-known approaches to autonomous driving—prominently the award winners of the DARPA Urban Challenge 2007—feature a considerable level of discretization. Examples include the use of a limited set of velocity profiles for the ego vehicle [10], a limited set of states [8, 4] and the use of dedicated systems for particular driving tasks [10, 8, 13, 1] that hand over responsibility among themselves based on a finite situation classification [13, 8], as well as a separation between path planning and vehicle control

[10, 1, 7, 2]. Another common case of discretization is to limit the behavior of the ego vehicle to a finite set of path candidates [10, 8, 7, 12].

The aim of the SPARC concept is to propose an alternative that requires no explicit classification of the current driving state, and no discrete state transitions for the ego vehicle. The intended benefit of this approach is to take all goals into account simultaneously, from basic navigation over traffic rules and collision avoidance down to currently desirable control parameters. The number of influences is intentionally kept flexible by reducing every contributing aspect to a unified *penalty* model, that is conciliated by the common language of stochastic modeling. The internal software state of the ego vehicle can in theory be kept constant between regular travel, unusual situations and even emergencies, and therefore no high-level understanding of the situation is required—neither are explicit state transitions that would have to be triggered by a decision module. The purpose of this paper is to shed light on the possibilities and feasibility of this alternative rather than to conclude its superiority over discretized approaches.

3 Penalties in a Holistic Model

The SPARC concept uses a holistic *penalty* concept that aims to reconcile all factors that are meant to influence the behavior of the ego vehicle. These factors involve legal constraints, safety, comfort, efficiency and ecology. Some of these are subject to uncertainty while others apply deterministically. All soft constraints are reduced to such penalties, while hard constraints are reserved exclusively for physically impossible states. Penalties are chosen such that they are real numbers, where higher penalties denote less desirable states, and such that their sum or integral is a meaningful quantity as well.

Penalties can generally be divided into two distinct classes of certainty (cf. Tab. 1): Those involving uncertainty (which will be discussed in Section 3.1) require a measure of probability, which can be approximated objectively by a prediction process. Those that apply deterministically (such as speed limits or the loss of comfort due to a sharp braking maneuver) can be evaluated directly. Both however require a definition of how undesirable a certain state is. This definition effectively determines how the ego vehicle will trade off between (e.g.) comfort and collision avoidance. Such priorities are implicitly inherent to any human driver, but they lie in everybody's personal responsibility. Defining a general set of rules is not the scope of this paper—the ideas will be outlined on an (obviously deficient) exemplary definition.

Penalties can further be divided into distinct classes of influence (cf. Tab. 1): Those affected by the current situation and its possible development (as represented in $\mathbf{H}$) are called *outer penalties*. We further distinguish between *primary outer penalties* $\mathcal{P}^{\mathrm{I}}_{\mathrm{out}}[\,\boldsymbol{\xi}\,|\,\mathbf{H}\,]$, which are based on collision risks, and *secondary outer penalties* $\mathcal{P}^{\mathrm{II}}_{\mathrm{out}}[\boldsymbol{\xi}\,|\,\mathbf{H}\,]$, which represent localizable traffic rules, such as speed limits, or non-vital interactions, such as potholes or speed bumps. These penalties are often also uncertain because they rely on sensor measurements (as considered in step 3 of the SPARC concept) and possibly the prediction (step 4). Penalties that only relate to state transitions of the ego vehicle itself are called *inner penalties* $\mathcal{P}_{\mathrm{in}}[\,\boldsymbol{\xi}\,]$. Examples for these would be uncomfortably strong lateral or longitudinal accelerations or high fuel consumption. Minimization towards the optimal trajectory $\boldsymbol{\xi}^*$ will need to take into account all of these terms, although their influence in the trajectory calculation should clearly vary.

		deterministic	**probabilistic**
inner		fuel consumption	loss of friction
outer	**primary**	collision (e.g. trees)	collision (e.g. cars)
	secondary	traffic rule violation	collision (e.g. wild animals)

Table 1: Types of penalties along with an example for each combination.

$$\mathcal{P}[\,\boldsymbol{\xi}\,|\,\mathbf{H}\,] = \mathcal{P}_{\text{in}}[\,\boldsymbol{\xi}\,] + \mathcal{P}^{\text{I}}_{\text{out}}[\,\boldsymbol{\xi}\,|\,\mathbf{H}\,] + \mathcal{P}^{\text{II}}_{\text{out}}[\boldsymbol{\xi}\,|\,\mathbf{H}\,] \tag{2}$$

The *holistic representation* $\mathbf{H}$ is, in its most simple form, a mapping from space and time to scalar-valued, positive penalties

$$\mathbf{H} : X \times Y \times T \to \mathbb{R}_{\geqslant 0} \tag{3}$$

where X and Y are bounded intervals of 2D space around the ego vehicle (which is located at $\boldsymbol{x}_0 = [x_0, y_0]^\mathsf{T}$), and T is an interval from t_0 ("now") up to several seconds into the future. The value $\mathbf{H}(x, y, t)$ denotes the penalty of traversing the location $[x, y]^\mathsf{T} = \boldsymbol{x}$ at time t.

3.1 Expected Values for Penalties

To compute the penalty for a possible collision, expected values can be used. The penalty for traversing a point $\boldsymbol{x}$ where an obstacle is certain to be found depends only on the severity of the collision. Defining a severity penalty $\mathcal{P}_{\text{sev}}$ is an ethical, legal, economical and physical question and, for this very reason, far beyond the scope of this paper. To convey an intuition, the severity penalty is set to the kinetic energy of the impact for the examples in this paper; clearly this definition hardly satisfies the practical requirements and should not be taken as a proposal. The kinetic energy W_{kin} that one object of mass m and velocity $\boldsymbol{v}$ exerts on the ego vehicle at time t_{coll} is

$$W_{\text{kin}} = m\|\dot{\boldsymbol{\xi}}(t_{\text{coll}}) - \boldsymbol{v}_{\text{obj}}\|_2^2 =: \mathcal{P}_{\text{sev}}. \tag{4}$$

While its exclusive use has obvious shortcomings, having the kinetic energy contribute to the penalty is justified as the kinetic energy of the impact can be turned into deformation energy acting on the participants, and is thus a measure of damage inflicted. A more sophisticated discussion on the effect of kinetic energy on traffic accidents can be found in [9].

If the obstacle is not known to overlap with $\boldsymbol{\xi}(t_{\text{coll}})$ with certainty, then its occupancy probability at this place and time must influence the traversal penalty at $\boldsymbol{\xi}(t_{\text{coll}})$. The *expected penalty* for this particular collision c with probability $p(c)$ is $p(c) \cdot \mathcal{P}_{\text{sev}}(c)$. Here $p(c)$ is equal to the probability of the obstacle occupying $\boldsymbol{\xi}(t_{\text{coll}})$, since the traversal of the ego vehicle is the conditional premise (i.e. taken to be certain) for this evaluation. $\mathcal{P}_{\text{sev}}(c)$ needs to be approximated from the ego vehicle trajectory and the predicted target trajectory (as well as its mass). If a set of several collisions $C(\boldsymbol{\xi}(t_{\text{coll}}))$ may occur at $\boldsymbol{\xi}(t_{\text{coll}})$, these potential collisions can (as a gross simplification) be regarded as independent. Through this, the total expected penalty of traversing $\boldsymbol{\xi}(t_{\text{coll}})$ can be described as

$$E[\,\mathcal{P}_{\text{sev}}\,|\,\boldsymbol{\xi}(t_{\text{coll}})\,] = \sum_{c \in C(\boldsymbol{\xi}(t_{\text{coll}}))} p(c) \cdot \mathcal{P}_{\text{sev}}(c). \tag{5}$$

Even though the assumption of stochastic independence involves the possibility of two obstacles occupying the same position, it greatly simplifies the computation, because $E[\,\mathcal{P}_{\text{sev}} \,|\, \boldsymbol{\xi}(t_{\text{coll}})\,]$ can be computed as an independent sum over all observed obstacles and their trajectories.

3.2 Prediction of Occupancy Probabilities

The prediction of the traffic development in the near future is step 4 in the proposed SPARC concept. To determine the probability $p(c)$ of a collision at a given location (or equivalently the probability of an obstacle o occupying a position $\boldsymbol{x}$ at time t, $p_o(\boldsymbol{x}, t)$), requires a prediction process. Presented here is the prediction process for observed cars. The prediction assumes the cars to follow legal tracks (as opposed to driving in arbitrary, illegal patterns), but can represent uncertainty about speed changes and forks in their tracks, as well as inter-vehicle dependencies concerning their behavior (both not presented here).

3.2.1 Speed changes and the Kumaraswamy distribution

To efficiently represent arbitrarily fine speed changes, speed distributions are used. Given a statistical distribution of speeds e.g. on a particular street or in inner-city scenarios in general, a car can be modeled to pick a speed at random from this distribution. The resulting distribution of uncertainties in speeds can be integrated into a distribution of uncertainties in positions. While the model corresponds to the vehicle picking the new speed at t_0 and keeping it constant from then on, the uncertainty in its initial choice propagates through time and thus resembles the (more accurate but also much more costly) use of a stochastic differential equation (cf. Fig. 3 (a)).

The model for speed distributions proposed in this paper is the Kumaraswamy distribution (introduced in [6]), whose probability density function (PDF) p_{K} and cumulative distribution function (CDF) P_{K} are given by

$$p_{\text{K}}(x; a, b) = a\, b\, x^{a-1}\, (1 - x^a)^{b-1} \tag{6}$$

$$P_{\text{K}}(x; a, b) = 1 - (1 - x^a)^b \tag{7}$$

It is similar to the Beta distribution (see [3, p. 137]) in that it has two shape parameters, a and b (which are useful to represent varying speed distributions), and is defined on a double-bounded interval (which is useful to represent physical limits of speeds and to narrow down the prediction range). The usual domain for the Kumaraswamy distribution as given above is $[0, 1]$, but the distribution functions can easily be scaled to represent a suitable range of speeds.

Given a cumulative speed distribution $P(v_{\text{upper}})$ which represents the probability of the speed lying between $-\infty$ and v_{upper}, the cumulative position distribution (for a position s_{upper} along a given track) at time t can be computed by

$$P_t(s_{\text{upper}}) = P\left(\frac{s_{\text{upper}}}{t}\right). \tag{8}$$

The resulting density profile of positions is shown in Fig. 3, along with a possible interpretation of these densities as a trajectory density. Therefore speed changes are accounted

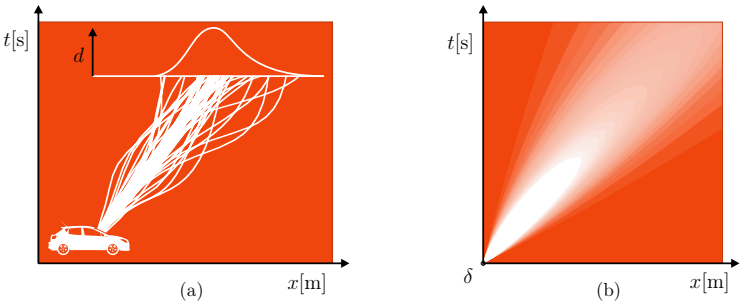

Figure 3: (a) Stochastic differential equation showing several possible trajectories for a car. (b) Approximation of the positional probability density by the Kumaraswamy distribution.

for in the prediction, even though an explicit stochastic differential equation is not set up. The occupancy probabilities along the track can thus be computed from a series of multiplications and sums given integral shape parameters to the Kumaraswamy distribution.

Setting the shape parameters depending on the state of the vehicles is beyond the scope of this paper; however, Fig. 5 shows the exemplary fitting of the Kumaraswamy distribution to German highway statistics, as a demonstration of its applicability. The data was taken from [5], as few applicable statistics are publicly available. In this publication the data was gathered by the German Federal Highway Research Institute (BAST) on German motorways (Autobahnen) in 1995, where no speed limits were given. Therefore the data is grouped by the expected speed at the respective locations of measurement (the three groups are shown in Fig. 5). Each cumulative distribution of measurements $M(v)$ was measured for $v \in V := \{80\,\mathrm{km\,h^{-1}}, 90\,\mathrm{km\,h^{-1}}, ..., 180\,\mathrm{km\,h^{-1}}\}$. Using linear least squares, a Kumaraswamy distribution CDF (with free parameters a and b and a domain of $[0\,\mathrm{km\,h^{-1}}, 180\,\mathrm{km\,h^{-1}}]$) was fitted to each of the three groups to satisfy:

$$P_K^* = \arg\min_{P_K} \sum_{v \in V} |P_K(v) - M(v)|^2 \tag{9}$$

The results are shown in Fig. 5 to demonstrate the applicability of the Kumaraswamy distribution for representing various speed distributions at a low computational effort.

4 Reaction Control

The 5$^{\text{th}}$ step of the proposed SPARC concept is the reaction control (RC) (cf. Fig. 1), which generates the trajectory based on the input of the SP block according to Eq. (1). The optimization is constrained by physical limits of the ego vehicle, but no further constraints are imposed. In particular it is not advised to introduce hard constraints to avoid collisions since this would limit the options in trading off between unavoidable collisions in extreme situations.

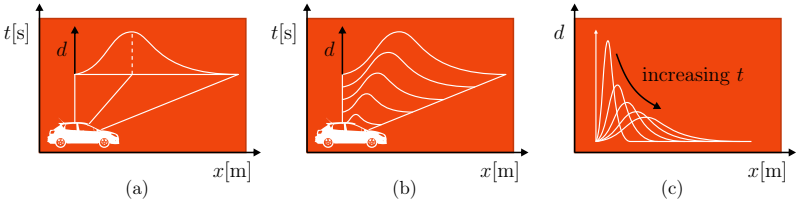

Figure 4: Speed distributions: (a) Connection between minimum speed, maximum speed and expected speed. (b) Family of probability distributions (density not to scale) by time. (c) Family of probability distributions (here: density to scale) converging to δ for $t \to 0$ (the leftmost "function" represented by an upward-pointing arrow).

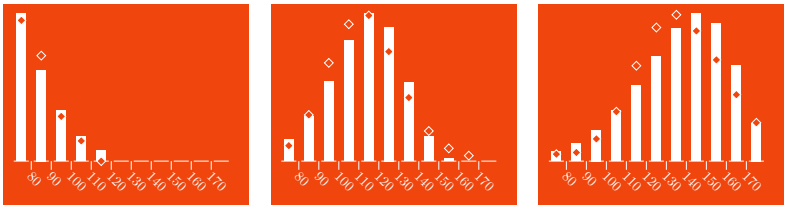

(a) Data group with expected velocity $E[v] = 50\,\mathrm{km\,h^{-1}}$, $a = 1.7786, b = 10.577$

(b) Data group with expected velocity $E[v] = 110\,\mathrm{km\,h^{-1}}$, $a = 7.14961, b = 26.8159$

(c) Data group with expected velocity $E[v] = 135\,\mathrm{km\,h^{-1}}$, $a = 6.23956, b = 4.35134$

Figure 5: Kumaraswamy distribution PDFs (bars) mapped to actual speed distributions (ticks) measured in [5] by linear least squares over the corresponding CDFs.

The results presented in Section 5 were produced using a variational approach. In this, the Euler–Lagrange equation (see [11, p. 33], [14, p. 48])

$$\frac{\partial \mathcal{P}[\boldsymbol{\xi}\,|\,\mathbf{H}]}{\partial \boldsymbol{\xi}} - \frac{\mathrm{d}}{\mathrm{d}t}\frac{\partial \mathcal{P}[\boldsymbol{\xi}\,|\,\mathbf{H}]}{\partial \dot{\boldsymbol{\xi}}} + \left(\frac{\mathrm{d}}{\mathrm{d}t}\right)^2 \frac{\partial \mathcal{P}[\boldsymbol{\xi}\,|\,\mathbf{H}]}{\partial \ddot{\boldsymbol{\xi}}} \equiv \mathbf{0} \tag{10}$$

is used for a gradient descent from an initial $\boldsymbol{\xi}^{(0)}$ which satisfies the following properties:

- The spatial components follow the path $\boldsymbol{\xi}^{(0)}$ which avoids permanent obstacles (such as walls or road limits) but intentionally does not take dynamic or unexpected obstacles (such as the shopping cart in Sec. 5 / Fig. 7) into consideration. It thus represents the characteristics of an offline map.
- The initial speed profile is the linear speed interpolation between the current speed $\dot{\boldsymbol{\xi}}(t_\mathrm{b})$ and target speed $\dot{\boldsymbol{\xi}}(t_\mathrm{e})$.

5 Practical Results

The methods presented here were evaluated in CarMaker, a commercial simulation software by IPG for driver assistance systems and vehicle dynamics. The trajectory optimization was performed in MATLAB. The dynamic traffic situations were modeled based on video footage, the static traffic situations were composed manually following requirements by Valeo.

Figure 6 shows the dynamic case of an intersection example. The ego vehicle is entering an intersection to take a left turn. Two cars (c_1 and c_2) are approaching the intersection on the opposite lane. They have the right of way, but the ego vehicle can decide to pass before or after them, or even in between, given that the spacing between c_1 and c_2 is adequately wide. The methods proposed herein allow to gauge the risks involved in such a maneuver and execute it if they are considered sufficiently low.

The uncertainty of c_1 and c_2 spreads visibly along the track in a "cloud" shape, due to uncertainties in future speed. As there is only one legal lane for both cars (their current lane), certainty about their lateral position is high. c_2 has a right turn indicator set and is thus predicted to turn right, as indicated by its cloud. c_1 is predicted to pass straight through the intersection. If the planning space for the ego vehicle is limited to its legal path, only the progress parameter s along the path needs to be optimized. The 3D planning problem ($x \times y \times t$) turns into a 2D planning problem ($s \times t$), indicated in Fig. 6(b) and used in Figs. 6(c—e). The relevant extracts of $\mathbf{H}$ (cut out along the given path) are shown (along with arrows denoting the most likely paths for c_1 and c_2 up to the point of intercept).

Figures 6(c—e) show the effect of spacing between c_1 and c_2: If the spacing is wide enough (Fig. 6(c)) the ego vehicle plans to pass between them. If the spacing is too narrow, the best solution is to wait until both cars have passed (Fig. 6(d)). The solutions are compared in Fig. 6(e). Everything shown in Fig. 6 represents a single time step in the real world. The very next control commands to follow the calculated trajectory are executed and the process steps are repeated (one quarter of a second later in our simulation). In the examples presented here, the ego vehicle passed collision-free through the oncoming traffic.

To contrast the dynamic case, Fig. 7 shows a static example typical of a simple valet parking application: A static obstacle (here: a shopping cart) needs to be avoided. For this, the trajectory is replanned along the two spatial coordinates. As the example is static, prediction is not a relevant influence. The spatial planning is constrained by the minimum turn radius of the ego vehicle. The simulation results in a collision-free passage around the shopping cart. If the walls (represented by traffic cones) are too narrow for the ego vehicle to drive around the shopping cart, the ego vehicle stops before it.

6 Conclusions and Outlook

The approach presented in this paper is currently in an early simulation stage, since several process steps need to be triggered manually. Therefore the amount of simulation examples is very limited. However these examples do suggest that it is possible to use the given methods for planning trajectories in autonomous driving which take the environment, traffic rules and vehicle dynamics into account at the same time. Work towards a more

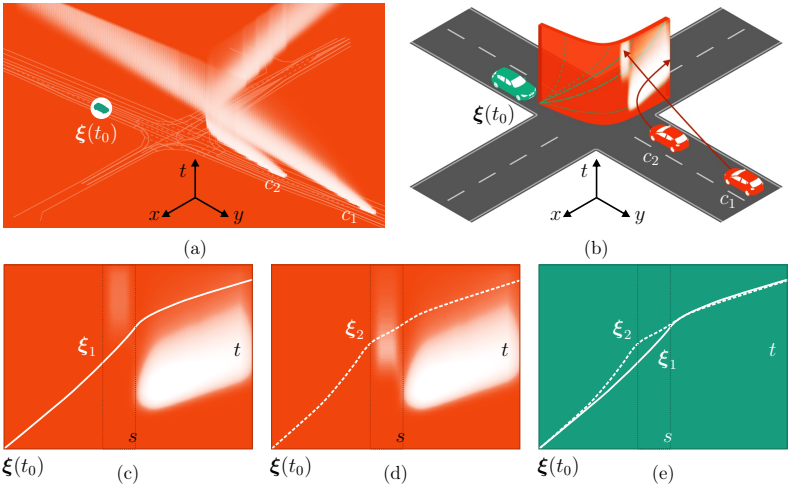

Figure 6: Example of the SPARC concept applied to an intersection, where the ego vehicle (green) located at $\boldsymbol{\xi}(t_0)$ wants to take a left turn through oncoming traffic (red), consisting of two cars c_1 and c_2. (a) Resulting energy cube (isometric perspective; vertical axis: t). (b) Schematic view (not to scale with (a)), cut-out of $\mathbf{H}$ along a given path and arrows (dark red) indicating most likely trajectories of c_1 and c_2. (c) Cut-out of $\mathbf{H}$ for wide gap between c_1 and c_2. (d) The same for a narrow gap. (e) Comparison of trajectories obtained in (c) and (d). In (c—e) the s boundaries of the opposite lane are indicated by the dashed vertical lines, to highlight the transition interval.

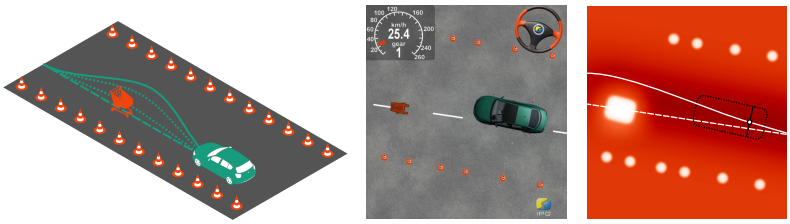

Figure 7: Example of the SPARC concept applied to a valet parking example, where the ego vehicle (green) needs to avoid a shopping cart (red). (a) Schematic view (not to scale) of original path (dashed), intermediate iteration results (dotted) and optimal trajectory (solid). (b) Situation as simulated in CarMaker. (c) Situation with initial trajectory (dashed) and optimal trajectory (solid) as obtained in MATLAB. The ego vehicle and its rear axis are shown in black.

extensive automation is underway that will allow for a more systematic evaluation in various traffic situations. The same applies to parameter estimation for the Kumaraswamy distribution.

The methods were chosen with a real-time implementation in mind. In particular, methods were preferred that confine themselves to multiplication and addition, as featured in dedicated hardware such as multiply–accumulate blocks, as well as methods that exhibit a high degree of parallelity to be exploited in hardware implementations, while retaining flexibility and expressiveness. As currently little optimization was performed, reliable figures on the computational effort cannot be given yet and remain to be produced. In particular, a hardware implementation has to be specified.

The concept remains valid in theory for any level of detail in a dynamic map—however, its usefulness is questionable with highly uncertain data (e.g. just point clouds of obstacles, no interpretation) or highly certain data (mostly fully automated vehicles communicating state and intentions via Car2Car). A more sophisticated assessment of applicability has yet to be developed.

Further techniques, such as Non-Linear Model Predictive Control (NMPC), as well as graphical models for prediction and trajectory planning, are currently under evaluation but lie beyond the scope of this paper. All approaches have parameters that depend on statistical data and/or factual data such as vehicle limits and traffic rules. Determining methods to set these parameters adequately will be mandatory to apply the techniques to real-world situations.

Acknowledgements

This work was partially supported by Valeo Schalter und Sensoren GmbH within the V50 project, and by the Fraunhofer-Gesellschaft along with the state of Baden-Württemberg within their joint innovation cluster REM 2030.

References

[1] A. Bacha, C. Bauman, R. Faruque, M. Fleming, C. Terwelp, C. Reinholtz, D. Hong, A. Wicks, T. Alberi, D. Anderson, S. Cacciola, P. Currier, A. Dalton, J. Farmer, J. Hurdus, S. Kimmel, P. King, A. Taylor, D. V. Covern, and M. Webster. Odin: Team VictorTango's entry in the DARPA Urban Challenge. *Journal of Field Robotics*, 25(8):467–492, 2008.

[2] J. Bohren, T. Foote, J. Keller, A. Kushleyev, D. Lee, A. Stewart, P. Vernaza, J. Derenick, J. Spletzer, and B. Satterfield. Little Ben: The Ben Franklin Racing Team's Entry in the 2007 DARPA Urban Challenge, 2008.

[3] M. G. Bulmer. *Principles of Statistics*. Dover Publications, 2nd edition, 1979.

[4] Y.-L. Chen, V. Sundareswaran, C. Anderson, A. Broggi, P. Grisleri, P. Porta, P. Zani, and J. Beck. TerraMax: Team Oshkosh Urban Robot. In M. Buehler, K. Iagnemma, and S. Singh, editors, *The DARPA Urban Challenge*, volume 56 of *Springer Tracts in Advanced Robotics*, pages 595–622. Springer Berlin Heidelberg, 2009.

[5] G. Kellerman. Geschwindigkeitsverhalten im Autobahnnetz 1992. *Straße + Autobahn*, 05 1995.

[6] P. Kumaraswamy. A generalized probability density function for double-bounded random processes. *Journal of Hydrology*, 46(1-2):79–88, March 1980.

[7] J. Leonard, J. How, S. Teller, M. Berger, S. Campbell, G. Fiore, L. Fletcher, E. Frazzoli, A. S. Huang, S. Karaman, O. Koch, Y. Kuwata, D. Moore, E. Olson, S. Peters, J. Teo, R. Truax, M. Walter, D. Barrett, A. Epstein, K. Maheloni, K. Moyer, T. Jones, R. Buckley, M. Antone, R. Galejs, S. Krishnamurthy, and J. Williams. A Perception Driven Autonomous Urban Robot. *International Journal of Field Robotics*, 25(10):727–774, 2008.

[8] M. Montemerlo, J. Becker, S. Bhat, H. Dahlkamp, D. Dolgov, S. Ettinger, D. Haehnel, T. Hilden, G. Hoffmann, B. Huhnke, D. Johnston, S. Klumpp, D. Langer, A. Levandowski, J. Levinson, J. Marcil, D. Orenstein, J. Paefgen, I. Penny, A. Petrovskaya, M. Pflueger, G. Stanek, D. Stavens, A. Vogt, and S. Thrun. Junior: The Stanford Entry in the Urban Challenge. *Journal of Field Robotics*, 2008.

[9] A. Sobhani, W. Young, D. Logan, and S. Bahrololoom. A kinetic energy model of two-vehicle crash injury severity. *Accident Analysis & Prevention*, 43(3):741 – 754, 2011.

[10] C. Urmson, J. Anhalt, H. Bae, J. A. D. Bagnell, C. R. Baker , R. E. Bittner, T. Brown, M. N. Clark, M. Darms, D. Demitrish, J. M. Dolan, D. Duggins, D. Ferguson , T. Galatali, C. M. Geyer, M. Gittleman, S. Harbaugh, M. Hebert, T. Howard, S. Kolski, M. Likhachev, B. Litkouhi, A. Kelly, M. McNaughton, N. Miller, J. Nickolaou, K. Peterson, B. Pilnick, R. Rajkumar, P. Rybski, V. Sadekar, B. Salesky, Y.-W. Seo, S. Singh, J. M. Snider, J. C. Struble, A. T. Stentz, M. Taylor , W. R. L. Whittaker, Z. Wolkowicki, W. Zhang, and J. Ziglar. Autonomous driving in urban environments: Boss and the Urban Challenge. *Journal of Field Robotics Special Issue on the 2007 DARPA Urban Challenge, Part I*, 25(8):425–466, June 2008.

[11] B. Van Brunt. *The Calculus of Variations*. Springer, 2010.

[12] M. Wang, T. Ganjineh, and R. Rojas. Action annotated trajectory generation for autonomous maneuvers on structured road networks. In 5^{th} *International Conference on Automation, Robotics and Applications (ICARA), 2011*, pages 67–72, 2011.

[13] J. M. Wille, F. Saust, and M. Maurer. Segmentübergreifende Bahnplanung mittels eines analytischen Optimierungsverfahrens für die autonome Fahrzeugführung auf dem Braunschweiger Stadtring. In *6. Workshop Fahrerassistenzsysteme – FAS 2009*, 2009.

[14] J. R. Ziehn. Energy-based collision avoidance for autonomous vehicles. Master's thesis, Leibniz Universität Hannover, Germany, October 16^{th} 2012.